Supporting Information

Nucleation Kinetics and Structure Evolution of Quasi-Two-Dimensional ZnO at Air-Water Interface: An *In situ* Time-Resolved Grazing Incidence X-ray Scattering Study

*Ziyi Zhang,[1] Corey Carlos,[1] Yizhan Wang,[1] Yutao Dong,[1] Xin Yin,[1] Lazarus German,[1] Kelvin Jordan Berg,[1] Wei Bu,[2] Xudong Wang[1,]**

[1]Department of Materials Science and Engineering, University of Wisconsin-Madison, Madison, Wisconsin 53706, United States

[2]NSF's ChemMatCARS, Pritzker School of Molecular Engineering, University of Chicago, Chicago, Illinois 60637, United States

**Corresponding author: Xudong Wang, Email: xudong.wang@wisc.edu*

Section 1. Experimental Section

Materials. All chemicals were purchased through Sigma-Aldrich and used without further purification.

ZnO nanosheets synthesis. All nanosheets were synthesized in a custom ILE chamber with a similar procedure based on the reported literature.[1,2] Different from most previous ILE growth of oxide NSs, a lower concentration was used here to slow down the crystal formation, especially for the nucleation stage. The precursor solution was prepared as 1 mM zinc nitrate ($Zn(NO_3)_2$) and 1 mM hexamethylenetetramine (HMTA) by dissolving 29.8 mg $Zn(NO_3)_2 \cdot 6H_2O$ and 14.0 mg HMTA in 100 mL deionized water. The solution was transferred into a Teflon trough (L-100mm, W-60mm, H-15mm) in the growth chamber for *in situ* measurements. Then 24 μL chloroform solution containing 1.8 mM sodium oleylsulfate (SOS) was dropwise dispersed on the solution surface to form an anionic monolayer. Subsequently, the trough was heated up to 60°C and the chamber was sealed and purged with helium at 5 psi for 5 min. The rest of the synthesis was in the environment with helium pressure at 1 psi. In addition, several key growth conditions were used in the *in situ* synthesis, including different surfactant amounts of 24 μL, 48 μL and 72 μL; different

precursor concentrations of 1, 5, 12.5 and 25 mM; and different solution temperatures of 60 °C and 70 °C.

***In situ* time-resolved grazing incidence synchrotron X-ray scattering measurements.** All liquid interface GID and GIXOS measurements were performed on Sector 15, NSF's ChemMatCARS, at Advanced Photon Source of Argonne Nation Laboratory to study the NS structure formation and crystal growth in real-time. To achieve *in situ* monitoring of the entire process of the ILE ZnO NSs growth, a compatible custom *in situ* ILE growth chamber was developed and integrated with the on-line liquid interface scattering instrument. The wavelength of monochromatic X-ray was 1.23984 Å (10 keV), and the scattering intensity was detected by a Dectris PILATUS 100 detector with 10 s exposure time for each image. 1D-pinhole mode was applied to GID that significantly improved the data collection efficiency without sacrificing angular resolution, which allows us to capture sample structure in a short time interval, down to 10 seconds. The measurements were continuously collected in a repeating sequence of a liquid surface focus height adjustment, GIXOS measurements (10 x 10s scans), a liquid surface focus height adjustment and GID measurements (3 x 10s scans) until the liquid surface below the trough edge (about 120 min). The sample growth chamber was purged with helium to minimize air scattering[3,4] and was kept warm under IR lamps

to remove water vapor condensation on the X-ray path. The growth time was started to count at the point of adding the surfactant on the solution surface. (Due to a beam-drop during the *in situ* measurement of the 5 mM sample, the diffractions could not be detected in the first ~40 min synthesis period.)

Other characterizations. The morphological SEM images were obtained from a Zeiss LEO 1530 Schottky-type field-emission scanning electron microscope.

Section 2. GID data processing method

The rare GID image directly collected from the PILATUS detector contains many types of backgrounds (**Fig. S1a**). A necessary data process was done before analysis. The purpose of the process is to remove the backgrounds and the unexpected scattering from the environment, such as the scattering from the atmosphere and moisture (humidity and condensation on Kapton window). GID images were collected by an area detector and were presented in the Q_{xy}-Q_z plane of the reciprocal space. Different from the regular X-ray diffraction patterns of bulk samples, the features from a crystalline surface or a 2D crystalline material are diffraction rods with intensity maximums at Q_z~0 and decaying along the Q_z-direction, which are also known as Bragg's rods.[5,6] By integrating the GID intensity along Q_z-direction, we can get linear XRD results in Q_{xy}-direction (also known as Q_z cut). In addition to the typical XRD background subtraction, a moisture background identifying and subtracting procedure is needed. The scattering signals from moisture have a specification uniform intensity distribution along all Q_z angles, which is shown as a rectangular shape background on the image. Therefore, they could be identified by comparing the intensity between low Q_z range and high Q_z range (**Fig. S1b**). In high Q_z range, diffraction signals

from ZnO NSs are weak, and water moisture backgrounds maintain the same intensity as it in low Q_z range. Then we have clean diffraction peaks for analysis (**Fig. S1c**). From the GID Q_z cut, we can get diffraction peak location, symmetry, intensity and FWHM, which are corresponding to the crystal lattice spacing distance, dimension, total sample amount and average domain size, respectively. The average lateral single-crystalline domain size (D) of the NSs could be calculated from FWHM of the 2D diffraction peak by applying Scherrer equation ($D = 0.89*2\pi/\Delta q$) with the X-ray wavelength of 1.23984 Å.[7,8] Unfortunately, the GID has an instrumentation resolution of 0.006 $Å^{-1}$, meaning any single-crystalline domains larger than 100 nm could not be accurately quantified. Since the NS domain sizes were substantially larger than 100 nm, only a qualitative relationship could be determined.

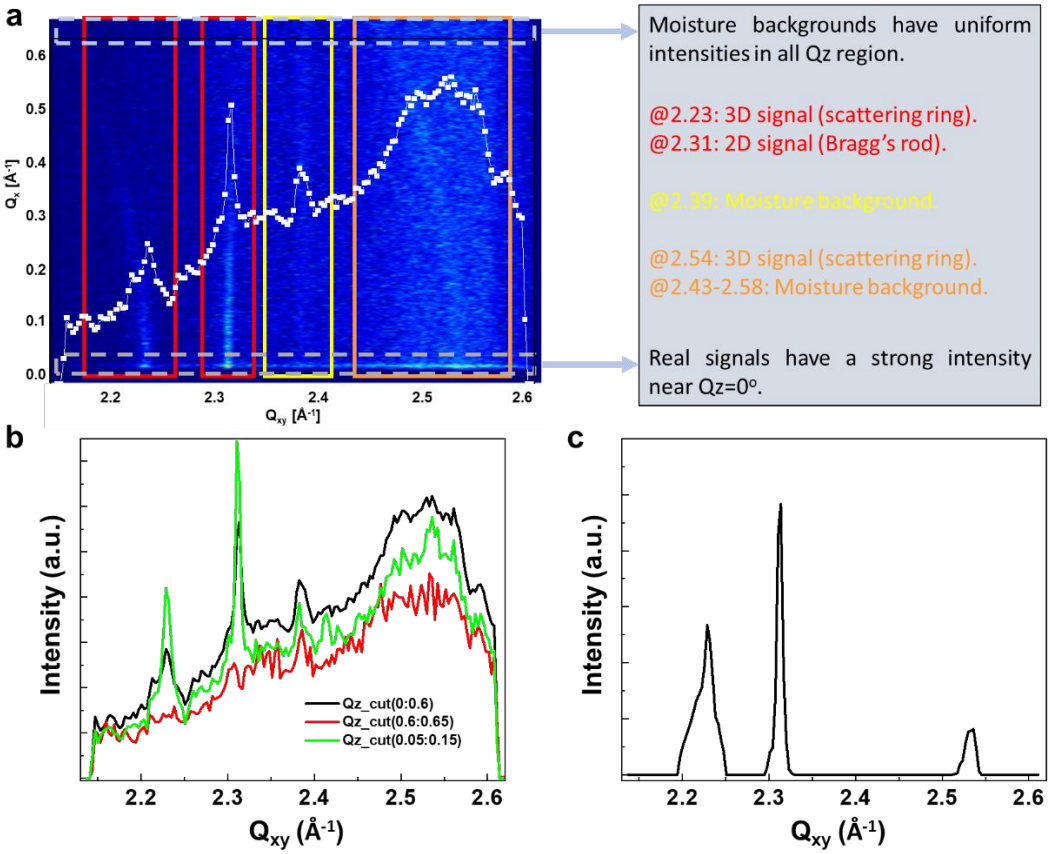

Figure S1. GID data processing method. **(a)** An original GID image taken from a Pilatus area detector showing the diffraction by ZnO NSs and water moisture. **(b)** Q_z cuts of the GID image with different integration Q_z ranges. **(c)** Processed GID peaks without backgrounds.

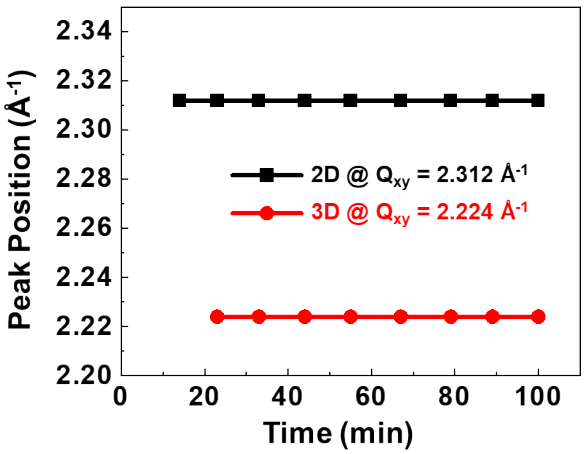

Figure S2. Diffraction peak positions in the crystal growth. [Measurement was done at 60°C with 1 mM Zn^{2+}].

Section 3. Nanosheet thickness calculation from fitting the periodicity of the GIXOS curve

GIXOS measures the intensity of off-specular diffuse scattering that provided the surface structure factors with a spatial resolution comparable to X-ray reflectivity and with a sub-minute temporal resolution. The intrinsic surface structure factor is shown as the electron density profile along the Q_z-direction which is normal to the air-water interface. It is similar to the curve taken from X-ray reflection (XR). The biggest advantage of GIXOS is the short measure time (~min), allowing us to know the kinetics at the interface. However, because GIXOS is a fast technique, it has lower Q_z resolution and much larger fluctuation compared to regular XR curves that GIXOS signal is much noisier and may lose some fine features. Theoretically, we could get the layered structure along the z-axis, including thickness and roughness, from a good fitting of GIXOS curve. However, due to the liquid surface fluctuations, and the scattering/absorption from water in this dynamic system, it is hard to fit the GIXOS curve with XR fitting algorithms or models. The practical way we can achieve at this moment is to assume the charge density of surfactant monolayer is much lower than the charge density of the ZnO crystalline NSs, so we could consider the oscillation periodicity reflecting the ZnO NS thickness. We manually identified the major periodicity and calculated the

nanosheet thickness from the average of a few periods. **Figure S3** shows the major vertical layered structure at the air-water interface which is directly related to the thickness of the ZnO NSs.

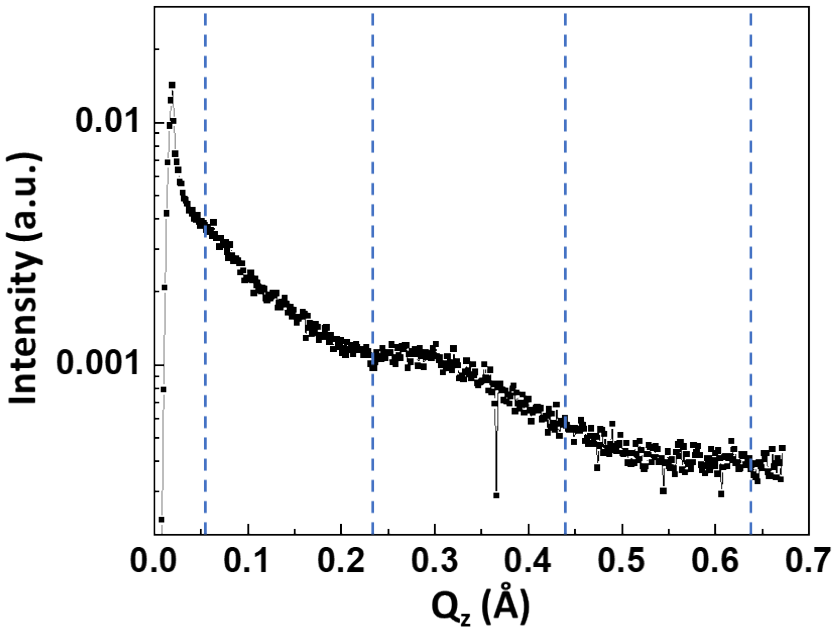

Figure S3. A rare GIXOS curve showing the vertical layered structures at air-water interface. Major periodicity ΔQ_z=31.7Å is marked by the dash lines.

Section 4. Packing density calculation at the air-water interface

Density of Zn atoms (ρ_{Zn}) in wurtzite ZnO:

At the air-water interface, Zn atoms have the HCP structure in wurtzite ZnO (0001) plane. Therefore, the lattice parameter (a_{Zn_2D}) can be calculated from the diffraction rod position (Q_{rod} = 2.312 Å) we obtained by applying the following equation:

$a_{Zn\_2D} = (2\pi/2.312\ \text{Å})/(\sqrt{(3)}/2) = 3.138$ Å.

Then, the density of Zn atoms (ρ_{Zn}) in wurtzite ZnO (0001) plane is:

$\rho_{Zn} = 1/[a_{Zn}^2 \cdot (\sqrt{(3)}/2] = 1/[(3.138\ \text{Å})^2 \cdot (\sqrt{(3)}/2] = 0.1085\ \text{Å}^{-2}$.

Density of SOS molecules (ρ_{SOS}) at air-water interface:

The SOS concentration (C) in chloroform solution is 1.8 mM, and the trough top area (A_{trough}) is 60 cm^2. The density of SOS molecules (ρ_{SOS}) at air-water interface can be calculated:

$\rho_{sos} = (C \cdot V \cdot N_A)/A_{trough} = (1.8 \cdot 10^{-3}$ mol/L) $\cdot$ (V_{sos} [μL] $\cdot 10^{-6}$ L) $\cdot$ ($6.022 \cdot 10^{23}$ /mol) / 60 $cm^2 = 1.8066 \cdot 10^{13}$ V $cm^{-2} = 0.0018066$ V $Å^{-2}$

Table. S1 Calculated surfactant density at air-water interface.

SOS solution amount (μL)	SOS molecule density at interface ($Å^{-2}$)
24	0.04336
48	0.08672
72	0.1301

*($\rho_{24\mu L\ SOS} < \rho_{48\mu L\ SOS} < \rho_{Zn} < \rho_{72\mu L\ SOS}$)

Section 5. Temperature effects in ILE ZnO NSs growth

While the NS formation temperature window was narrow, we managed to synthesize ZnO NSs at a raised solution temperature of 70 °C. As shown in **Figure S4a-c**, nucleation and growth were both faster at 70 °C than at 60 °C, the nuclei size was bigger (smaller FWHM) leading to rapid grain expansion and re-alignment. It was also discovered that NSs from 70°C were thicker with a lower intensity from the 2D diffraction rod. Instead of receiving ZnO triangular NSs, a continuous thick film was formed at the water-air interface after the *in situ* experiment. This suggests that the morphology at higher temperatures was more irregular. Generally, increasing the synthesis temperature didn't improve the quality of the ZnO triangular NS morphology. Fast reaction kinetics attenuated the regulation from the surfactant monolayer and led to more 3D large nuclei to a thick continuous polycrystalline film. Higher temperature also impeded longer-time *in situ* observation due to a much faster solution evaporation, making the water level drop below the trough edge much quicker.

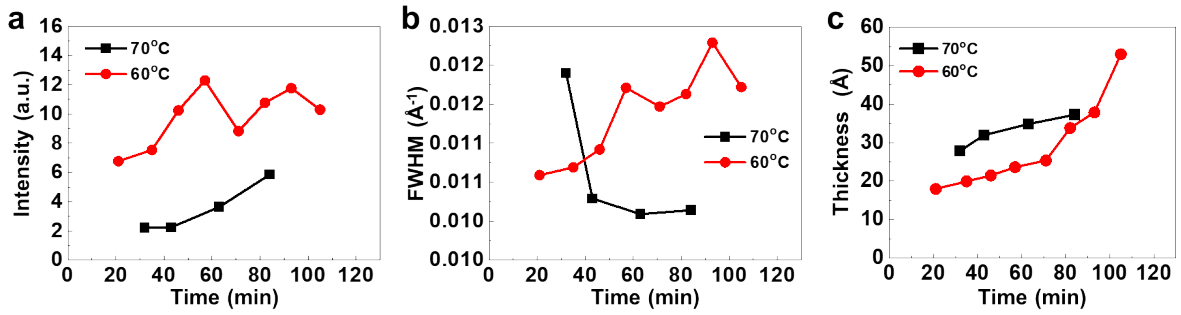

Figure S4. ZnO NSs crystallinity and thickness changes at different temperatures. **(a)** Diffraction rod (2D) intensity, **(b)** FWHM and **(c)** nanosheet thickness evaluation as a function of growth time at different growth temperatures [Measurements were done with 25 mM Zn^{2+} and 24 mL SOS].

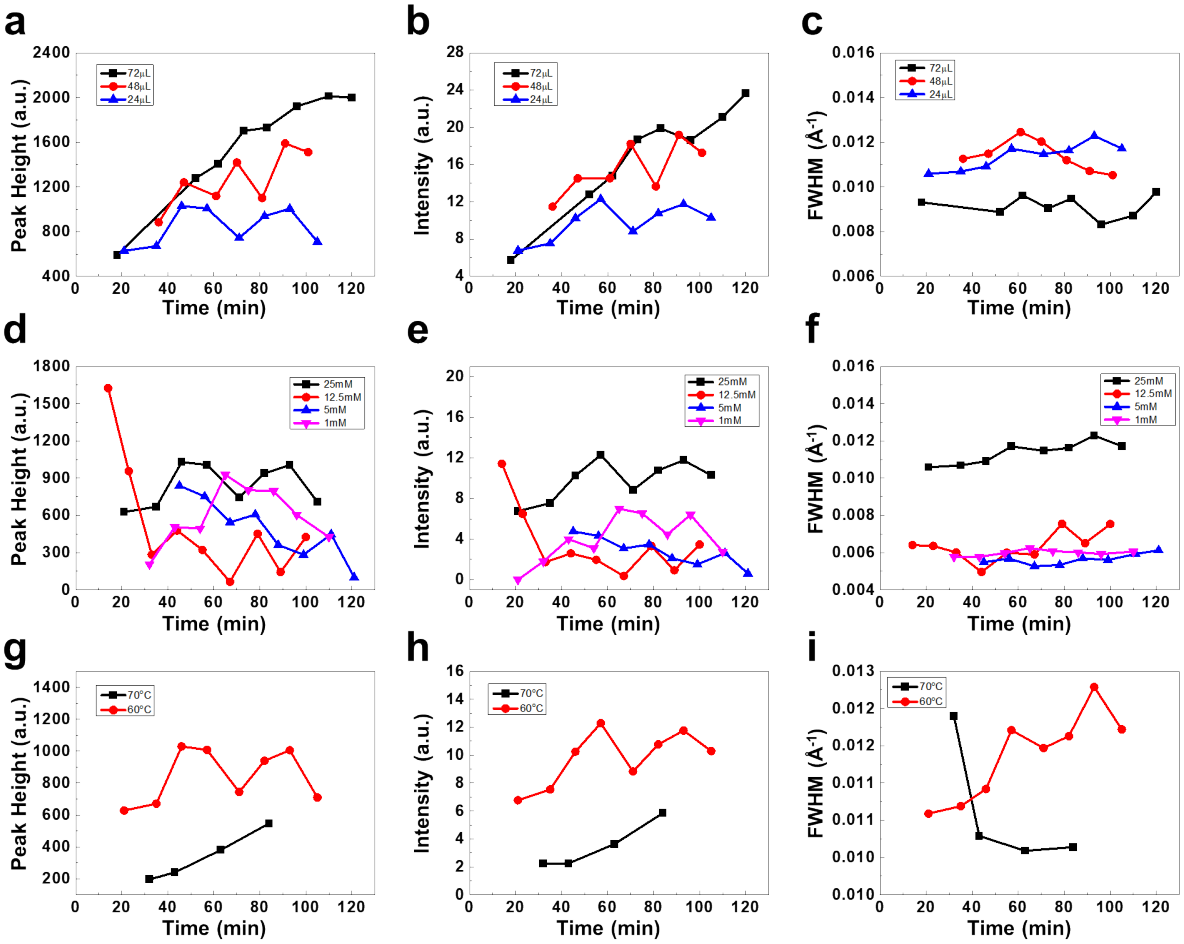

Figure S5. *In situ* GID of the surface 2D peak (Q_{xy}=2.312Å^{-1}) at different growth conditions. Different surfactant densities: **(a)** Peak height; **(b)** Peak intensity; and **(c)** FWHM. [Measurements were done at 60°C with 25mM Zn^{2+}]. Different Zn^{2+} ion concentrations: **(d)** Peak height; **(e)** Peak intensity; and **(f)** FWHM. [Measurements were done at 60°C with 24μL SOS]. Different temperatures): **(g)** Peak height; **(h)** Peak intensity; and **(i)** FWHM. [Measurements were done with 25mM Zn^{2+} and 24μL SOS].

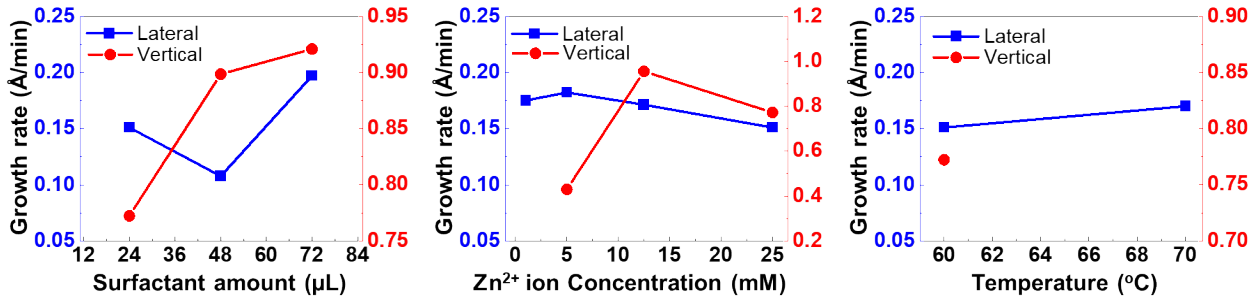

Figure S6. ZnO NSs thickness growth rates in lateral and vertical growth stages at different conditions obtained from the slopes of linear fittings.

REFERENCES

1 Wang, F. *et al.* Nanometre-thick single-crystalline nanosheets grown at the water–air interface. *Nature communications* **7**, 1-7 (2016).

2 Yin, X. *et al.* Unit cell level thickness control of single-crystalline zinc oxide nanosheets enabled by electrical double-layer confinement. *Langmuir* **33**, 7708-7714 (2017).

3 Nayak, S., Lovering, K., Bu, W. & Uysal, A. Anions Enhance Rare Earth Adsorption at Negatively Charged Surfaces. *The journal of physical chemistry letters* **11**, 4436-4442 (2020).

4 Hu, Q. *et al.* In situ dynamic observations of perovskite crystallisation and microstructure evolution intermediated from [PbI 6] 4− cage nanoparticles. *Nature communications* **8**, 1-9 (2017).

5 Tolan, M., Press, W., Brinkop, F. & Kotthaus, J. X-ray diffraction from laterally structured surfaces: Crystal truncation rods. *Journal of applied physics* **75**, 7761-7769 (1994).

6 Petukhov, A., Dolbnya, I., Aarts, D., Vroege, G. & Lekkerkerker, H. Bragg rods and multiple X-ray scattering in random-stacking colloidal crystals. *Physical review letters* **90**, 028304 (2003).

7 Ingham, B. & Toney, M. F. in *Metallic Films for Electronic, Optical and Magnetic Applications* (eds Katayun Barmak & Kevin Coffey) 3-38 (Woodhead Publishing, 2014).

8 Patterson, A. L. The Scherrer Formula for X-Ray Particle Size Determination. *Physical Review* **56**, 978-982, doi:10.1103/PhysRev.56.978 (1939).